



Article

# Unraveling the Binding Mechanism of Alzheimer's Drugs with Irisin: Spectroscopic, Calorimetric, and Computational Approaches

Rashid Waseem <sup>1</sup>, Anas Shamsi <sup>1</sup>, Tanzeel Khan <sup>1</sup>, Md. Imtaiyaz Hassan <sup>1</sup>, Syed Naqui Kazim <sup>1</sup>,  
Mohammad Shahid <sup>2</sup> and Asimul Islam <sup>1,\*</sup>

<sup>1</sup> Centre for Interdisciplinary Research in Basic Sciences, Jamia Millia Islamia, New Delhi 110025, India; rashid.waseem439@gmail.com (R.W.); anas.shamsi18@gmail.com (A.S.); aligbcb11@gmail.com (T.K.); mihassan@jmi.ac.in (M.I.H.); skazim@jmi.ac.in (S.N.K.)

<sup>2</sup> Department of Basic Medical Sciences, College of Medicine, Prince Sattam Bin Abdulaziz University, Al-Kharj 11942, Saudi Arabia; dr.shahid90@yahoo.com

\* Correspondence: aislam@jmi.ac.in

**Abstract:** The prevalence of Alzheimer's disease (AD) has been a major health concern for a long time. Despite recent progress, there is still a strong need to develop effective disease-modifying therapies. Several drugs have already been approved to retard the progression of AD-related symptoms; however, there is a need to develop an effective carrier system for the delivery of drugs to combat such diseases. In recent years, various biological macromolecules, including proteins, have been used as carriers for drug delivery. Irisin is a beneficial hormone in such diseases, including AD and related pathologies. Herein, the interaction mechanism of irisin with AD drugs such as memantine, galantamine, and fluoxetine is investigated. Fluorescence studies revealed that the above drugs bind to irisin with significant affinity, with fluoxetine having the highest binding affinity. Isothermal titration calorimetry (ITC) complemented the spontaneous binding of these drugs with irisin, delineating various associated thermodynamic and binding parameters. Molecular docking further validated the fluorescence and ITC results and unfolded the mechanism that hydrogen bonding governs the binding of fluoxetine to irisin with a significant binding score, i.e.,  $-6.3$  kcal/mol. We believe that these findings provide a promising solution to fight against AD as well as a platform for further research to utilize irisin in the drug-delivery system for an effective therapeutic strategy.

**Keywords:** irisin; molecular docking; fluorescence spectroscopy; drug delivery; Alzheimer's disease; isothermal titration calorimetry



**Citation:** Waseem, R.; Shamsi, A.; Khan, T.; Hassan, M.I.; Kazim, S.N.; Shahid, M.; Islam, A. Unraveling the Binding Mechanism of Alzheimer's Drugs with Irisin: Spectroscopic, Calorimetric, and Computational Approaches. *Int. J. Mol. Sci.* **2022**, *23*, 5965. <https://doi.org/10.3390/ijms23115965>

Academic Editor: Bruno Imbimbo

Received: 24 April 2022

Accepted: 23 May 2022

Published: 25 May 2022

**Publisher's Note:** MDPI stays neutral with regard to jurisdictional claims in published maps and institutional affiliations.



**Copyright:** © 2022 by the authors. Licensee MDPI, Basel, Switzerland. This article is an open access article distributed under the terms and conditions of the Creative Commons Attribution (CC BY) license (<https://creativecommons.org/licenses/by/4.0/>).

## 1. Introduction

Alzheimer's disease (AD) is the most prevalent neurological disease worldwide, pathologically characterized by late-stage amyloid  $\beta$  ( $A\beta$ ) plaques, neurofibrillary tangles (NFTs), and neuronal cell death [1]. Around 50–55 million people worldwide are known to be affected by dementia, including AD, and it is predicted that its prevalence may reach up to 150 million by 2050 [2]. Many theories about the causes of AD exist, but the reason underlying its pathogenesis has not been understood completely; hence, there has been a hindrance in the development of new therapeutics for the cure of the AD. The accumulated  $A\beta$  plaques and NFTs caused by abnormally hyperphosphorylated tau protein are the pathological hallmarks of AD. The accumulation of  $A\beta$  plaques forms amyloid senile plaques (SPs), which, along with NFTs, have been intricately involved in the pathogenesis of AD [3]. It is believed that when  $A\beta$  peptides are produced excessively, they accumulate to form senile plaques resulting in neuronal death [3]. Over the last few years, AD treatment has mainly involved  $A\beta$ -targeting therapies, and various drug candidates targeting  $A\beta$  are also in clinical trials [2]. Along with  $A\beta$ , the tau pathway also has an important role in AD pathology and is receiving much attention for potential AD therapeutics [4].

Since AD has a multifactorial origin, current therapeutic approaches have not successfully addressed the root cause of its pathogenesis and are used for symptomatic treatment [5,6]. Although many drug candidates targeting A $\beta$  and tau pathology are in the clinical phase, they provide only limited symptomatic relief. None can effectively slow down or halt the disease's progression. Most of the drugs that have been approved for symptomatic treatment of mild to moderate dementia in AD and associated pathologies work mainly on the N-Methyl-D-Aspartate (NMDA) receptor or the cholinergic pathway [7]. Since synaptic dysfunction and memory impairment are common features of AD pathogenesis, the restoration of synapse function and memory is important in AD management.

Developing an effective carrier system for drug delivery is essential to combat various diseases. Many drug carriers, including magnetic nanoparticles, hydrogels, liposomes, and microspheres, have been developed for the treatment and diagnosis of various diseases [8,9]. However, finding an appropriate drug carrier system is not an easy task. Drug carrier systems have several shortcomings; poor stability, the undesired release of drugs, low drug-loading content, high cost, and toxicity. A good drug carrier system should have specific properties such as non-immunogenicity, optimal bioavailability, the ability to target a specific site, and non-toxic behavior. Natural biological molecules such as proteins and polysaccharides have excellent drug carrier properties. In recent research, the paradigm of the drug carrier system has been shifting to the use of biological macromolecules to deliver therapeutic drugs. Many investigators use proteins such as silk fibroin, transferrin, and albumin for drug carrier systems [10–12]. Irisin is a newly identified hormone known to have a protective effect against synapse failure and cognitive decline in AD-related pathologies [13]. It has been reported that irisin is secreted in the heart, liver, pancreas, and testes, and it crosses the blood–brain barrier [13,14]. In the brain, irisin regulates brain-derived neurotrophic factor (BDNF) expression and helps in protecting the neuronal damage caused by oxidative stress [15,16].

Moreover, it has also been demonstrated that FNDC5/irisin interacts with the amyloid precursor protein (APP) and regulates A $\beta$  level in the brain [14,17]. Therefore, it is speculated that using irisin as a drug carrier for the drugs approved for AD-related pathology could be a promising strategy for treating AD. Memantine, galantamine, rivastigmine, etc., are some approved drugs for treating mild to moderate AD symptoms. Figure 1 shows the structure of all these drugs. Memantine is a non-competitive NMDA receptor antagonist, which protects neurons against the overstimulation of NMDA receptors in the case of AD [18,19]. Galantamine is a cholinergic drug that inhibits the acetylcholinesterase (AChE) enzyme and alters the nicotinic cholinergic receptors, thereby counteracting AD [20,21]. Fluoxetine is another FDA-approved drug, which is a selective serotonin reuptake inhibitor (SSRI) antidepressant. Fluoxetine exerts its action through inhibition of serotonin uptake by nerve cells (neurons) and helps people with anxiety, depression, or obsessive-compulsive symptoms [22,23]. Herein, we have studied the interaction between irisin and AD drugs (memantine, galantamine, and fluoxetine) implicated in treating AD-related pathology. We have employed fluorescence spectroscopy, ITC, and molecular docking to elucidate the interaction pattern of irisin with these drugs and to decipher the binding mechanism.

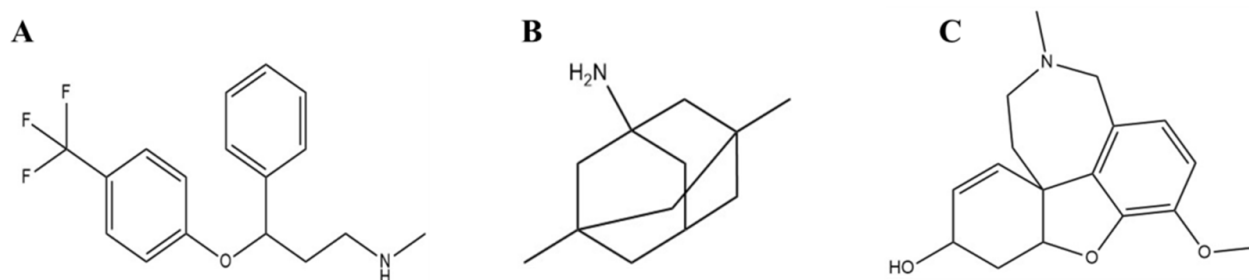


**Figure 1.** Two-dimensional structures of (A) Fluoxetine, (B) Memantine and (C) Galantamine.

## 2. Results and Discussion

### 2.1. Fluorescence Spectroscopic Measurements

Fluorescence spectroscopy is a commonly deployed technique for studying protein–ligand interaction, as it reveals various binding parameters as well as an understanding of the strength of the interaction [24]. Intrinsic fluorescence reveals information about the local microenvironment of aromatic amino acids, aiding in the investigation of the formation of the protein–ligand complex [25,26]. A decline in the fluorescence intensity of proteins with increasing ligand concentrations is termed fluorescence quenching [27].

Herein, the fluorescence quenching was observed for irisin–fluoxetine, irisin–memantine, and irisin–galantamine interactions. Fluorescence emission spectra of free irisin and irisin with different concentrations of fluoxetine (0–30  $\mu\text{M}$ ), memantine (0–24  $\mu\text{M}$ ), and galantamine (0–20  $\mu\text{M}$ ) are shown in Figure 2. The native irisin shows fluorescence emission maxima around 344 nm [28]. The fluorescence quenching of irisin was observed with increasing ligand concentrations for all three drugs. Fluorescence quenching was mathematically analyzed by applying (1) the Stern–Volmer (SV) and (2) double logarithmic equations to determine various quenching and binding parameters of protein–drug complexes as per previous reports [24,29].

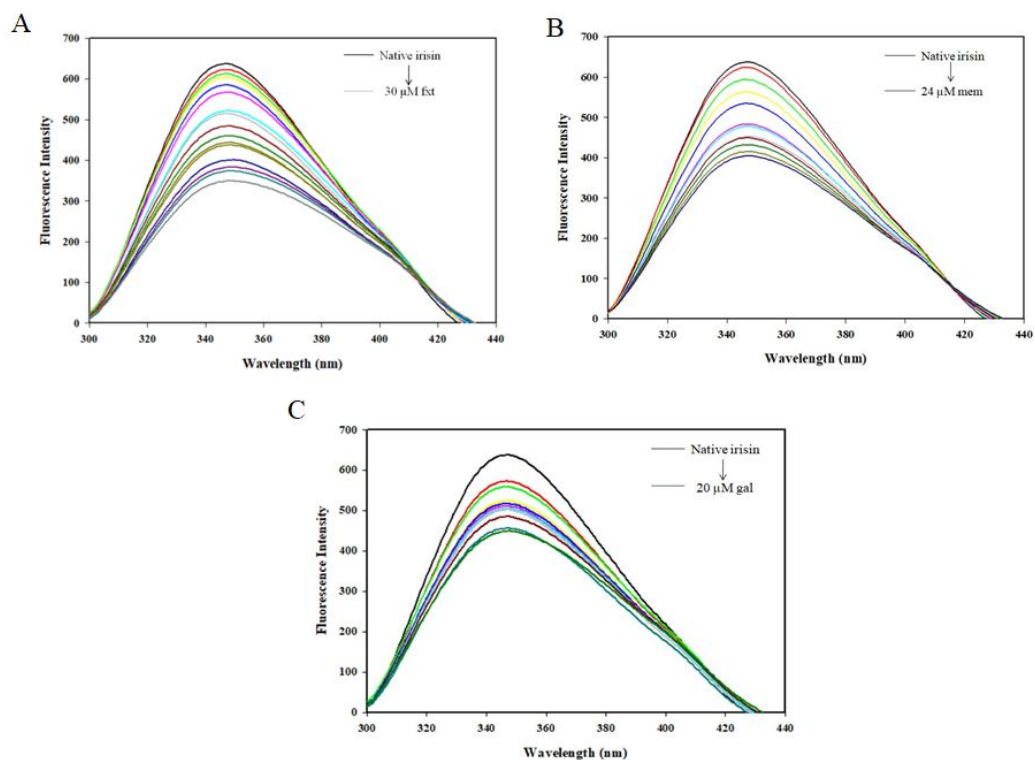


**Figure 2.** The fluorescence spectra of irisin in the presence of (A) Fluoxetine (0–30  $\mu\text{M}$ ), (B) Memantine (0–24  $\mu\text{M}$ ), and (C) Galantamine (0–20  $\mu\text{M}$ ).

$$\frac{F_0}{F} = 1 + K_{sv}[C] \quad (1)$$

$$\log \frac{F_0 - F}{F} = \log K + n \log [C] \quad (2)$$

where  $F_0$  refers to the intensity of free irisin and  $F$  is the intensity of irisin in the presence of the drug.  $[C]$  denotes the varying concentration of drugs.  $K_{sv}$  is the resulting Stern–Volmer constant.

$K$  refers to the “binding constant of the irisin–drug complex”,  $C$  is the drug concentration, and “ $n$ ” denotes the number of binding sites.

Figure 3 depicts SV plots of  $F_0/F$  on the  $y$ -axis and [Fluoxetine], [Memantine], and [Galantamine] on the  $x$ -axis. The slope of the SV plot gives the Stern–Volmer constant ( $K_{sv}$ ) value using the SV equation (Equation (1)), which was highest for the irisin–fluoxetine interaction, i.e.,  $2.77 \times 10^4 \text{ M}^{-1}$ . The values of the  $K_{sv}$  are listed in Table 1. To estimate the binding constants and number of binding sites, a double logarithmic plot (Equation (2)) was used [24]. The intercept of this plot provides the binding constant ( $K$ ), and the slope of this plot gives the number of binding sites ( $n$ ). Figure 4 depicts the double logarithmic plot for all three drugs, while Table 2 lists the binding parameters obtained. It was observed that fluoxetine binds to irisin with the highest affinity ( $K = 0.21 \times 10^7 \text{ M}^{-1}$  at  $25^\circ \text{C}$ ). Memantine and galantamine also showed significant binding to irisin, with a binding constant ( $K$ ) of  $9.78 \times 10^5 \text{ M}^{-1}$  and  $0.14 \times 10^3 \text{ M}^{-1}$ , respectively. Thus, it can be inferred that each of these AD drugs binds to irisin, forming a stable complex, with fluoxetine having the maximum affinity among the three drugs.

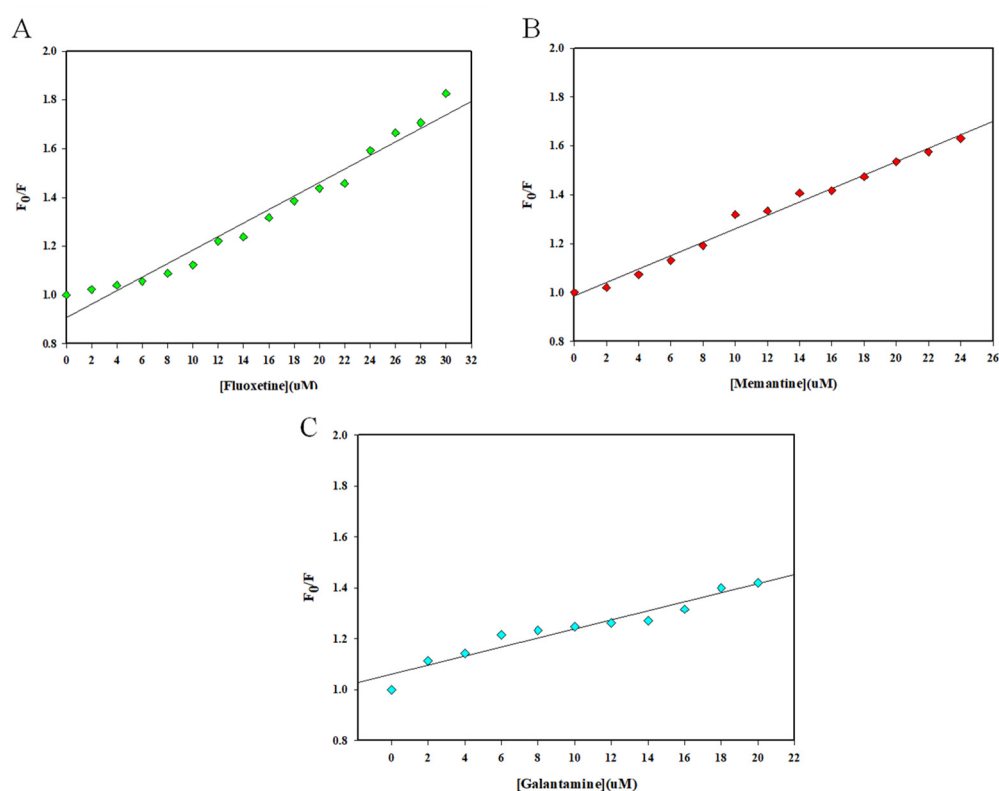


**Figure 3.** Stern–Volmer plot for the quenching of irisin fluorescence by (A) Fluoxetine, (B) Memantine, and (C) Galantamine.

**Table 1.** Values of Stern–Volmer quenching constants obtained from Stern–Volmer equation.

Irisin–Drug	$K_{sv}$ ( $10^4 \text{ M}^{-1}$ )	$R^2$
Irisin–Fluoxetine	2.77	0.97
Irisin–Memantine	2.73	0.98
Irisin–Galantamine	1.77	0.94

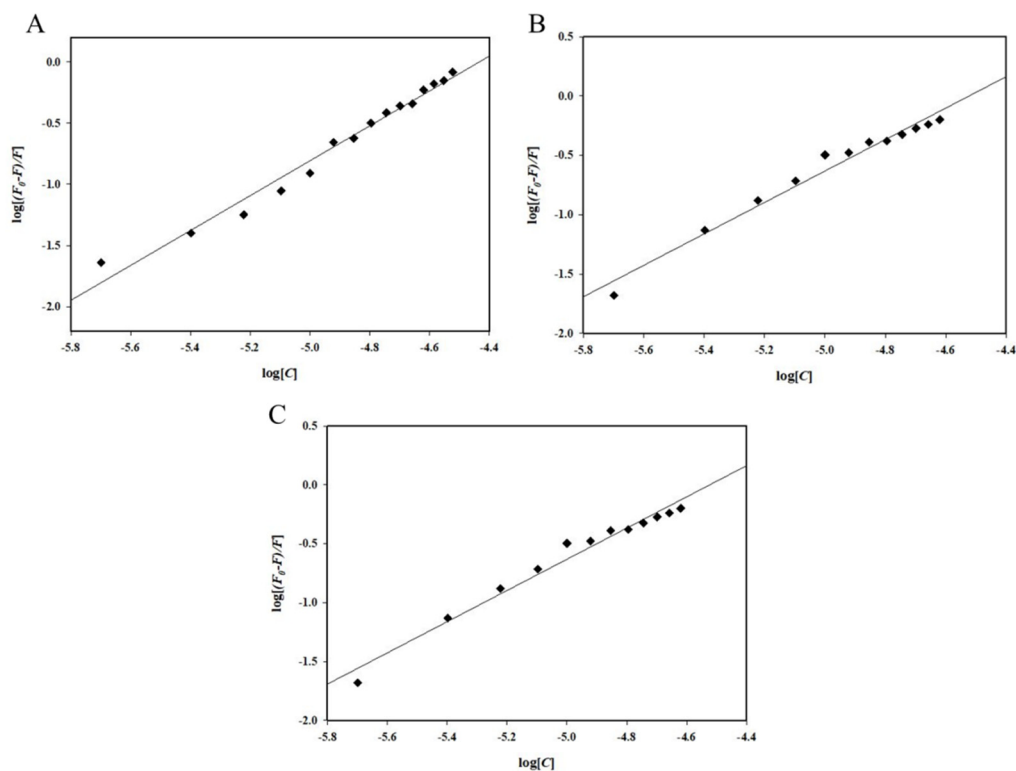


**Figure 4.** Double logarithmic plot for the quenching of irisin fluorescence by (A) Fluoxetine, (B) Memantine, and (C) Galantamine.

**Table 2.** Binding parameters obtained from double logarithmic equation.

Irisin–Drug	$K$	$n$
Irisin–Fluoxetine	$0.21 \times 10^7 \text{M}^{-1}$	1.43
Irisin–Memantine	$9.78 \times 10^5 \text{M}^{-1}$	1.32
Irisin–Galantamine	$0.14 \times 10^3 \text{M}^{-1}$	0.56

## 2.2. Isothermal Titration Calorimetry (ITC)

A complete description of the binding energetic was delineated by isothermal titration calorimetry, with a focus on achieving deeper insights into the interaction mechanisms of fluoxetine, memantine, and galantamine with irisin. ITC is a multidimensional approach that is routinely used to discover the protein–ligand system’s thermodynamic parameters and molecular forces involved in the binding processes [30]. The formation or dissociation of the protein–ligand complex results in either the release or the absorption of heat in the sample cell, which is measured for a reference cell filled with a corresponding buffer. The deduction of dilution heat corrected the results of the sequential titrations for all three ligands. The binding constant ( $K$ ), the number of binding sites ( $n$ ), entropy change ( $\Delta S$ ), and enthalpy change ( $\Delta H$ ) were determined directly by curve fitting [19]. Figure 5A–C shows the ITC isotherm obtained for irisin–fluoxetine, irisin–memantine, and irisin–galantamine. The upper panel demonstrates each peak in the isotherm representing a single injection of different ligands (fluoxetine, memantine, and galantamine) into the irisin solution. The lower panel depicts the integrated plot of heat released per injection as a function of molar ratio of ligand to the protein. It is clear from these isotherms that fluoxetine, memantine, and galantamine spontaneously bind to irisin, forming a stable complex. Additionally, the negative heat deflection for all three ligands suggests that the binding is an exothermic process. Table 3 shows different thermodynamic parameters obtained for the binding of ligands with irisin. ITC results further validated the fluorescence binding

observations, affirming the binding of fluoxetine, memantine, and galantamine with irisin, while fluoxetine showed the maximum affinity for irisin.

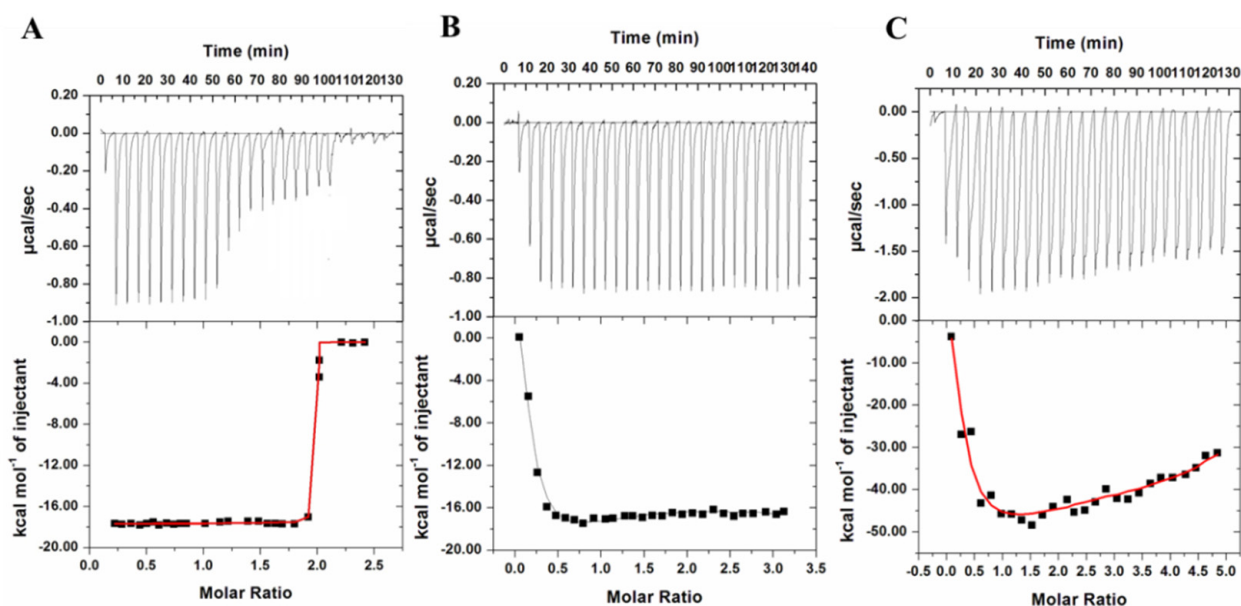


**Figure 5.** ITC profile of (A) Irisin–Fluoxetine, (B) Irisin–Memantine, and (C) Irisin–Galantamine systems. The top panels show raw data obtained upon sequentially titrating ligand into the protein of interest (irisin) present in the sample cell. The bottom panels show the binding isotherm obtained upon plotting the calorimetric titration’s integrated heat results after the correction of dilution heat against the molar ratio.

**Table 3.** Binding and thermodynamic parameters obtained from ITC.

Irisin–Fluoxetine System		
$K_a$ (Association Constant), $M^{-1}$	$\Delta H$ (Enthalpy Change), cal/mol	$\Delta S$ (cal/mol/deg)
$K_{a1} = 6.41 \times 10^6 \pm 9.66 \times 10^4$	$\Delta H_1 = -1.23 \times 10^4 \pm 979.4$	$\Delta S_1 = -10.3$
Irisin–Memantine system		
$K_{a1} = 8.97 \times 10^4 \pm 2.9 \times 10^3$	$\Delta H_1 = 5744 \pm 2.52 \times 10^3$	$\Delta S_1 = 41.9$
$K_{a2} = 1.07 \times 10^5 \pm 4.2 \times 10^3$	$\Delta H_2 = -1.357 \times 10^5 \pm 7.41 \times 10^3$	$\Delta S_2 = -432$
$K_{a3} = 9.91 \times 10^4 \pm 5.5 \times 10^3$	$\Delta H_3 = 1.92 \times 10^5 \pm 1.74 \times 10^4$	$\Delta S_3 = 669$
$K_{a4} = 1.06 \times 10^5 \pm 6.1 \times 10^3$	$\Delta H_4 = -1.99 \times 10^5 \pm 1.65 \times 10^4$	$\Delta S_4 = -645$
Irisin–Galantamine system		
$K_{a1} = 1.05 \times 10^5 \pm 1.7 \times 10^4$	$\Delta H_1 = 6763 \pm 6.18 \times 10^3$	$\Delta S_1 = 45.7$
$K_{a2} = 1.24 \times 10^5 \pm 2.3 \times 10^4$	$\Delta H_2 = -2.121 \times 10^5 \pm 3.19 \times 10^4$	$\Delta S_2 = -688$
$K_{a3} = 6.16 \times 10^4 \pm 9.1 \times 10^3$	$\Delta H_3 = 1.88 \times 10^5 \pm 6.12 \times 10^4$	$\Delta S_3 = 655$
$K_{a4} = 5.54 \times 10^4 \pm 1.0 \times 10^4$	$\Delta H_4 = -3.076 \times 10^5 \pm 4.49 \times 10^4$	$\Delta S_4 = -1.01 \times 10^3$

### 2.3. Molecular Docking

Molecular docking is a useful technique for obtaining mechanistic details of protein–ligand interactions at a molecular level, further supporting the identification of interacting residues and calculating affinity scores. This study utilized a blind docking approach to identify all possible interactions between irisin and different drugs. The results of blind docking of each compound, that is, all the potential binding sites determined for each compound have been shown in Figure S1. Additionally, their binding scores also have

been provided in Table S2. For the irisin–fluoxetine interaction, the predicted affinity score was estimated as  $-6.3$  kcal/mol, which is significant and affirms that fluoxetine is a possible binding partner of irisin. The docking analyses of memantine and galantamine with irisin also showed significant affinity, and the binding scores were  $5.7$  kcal/mol and  $-5.6$  kcal/mol, respectively. The docking analysis also supports the fluorescence and ITC results, which revealed that fluoxetine binds to irisin with the highest affinity. Figure 6 depicts the irisin in complex with docked fluoxetine, memantine, and galantamine shown in the ball-and-sticks model. Various interactions were shown by fluoxetine with key irisin residues, including one hydrogen bond with Gln103 and a few other non-covalent interactions. The 2D plot of the irisin–fluoxetine interaction showed a detailed analysis of all important residues of irisin interacting with fluoxetine (Figure 7A). Fluoxetine showed multiple van der Waals interactions with Ser65, Gln67, Arg75, Gln78, Val80, and His101 of irisin.

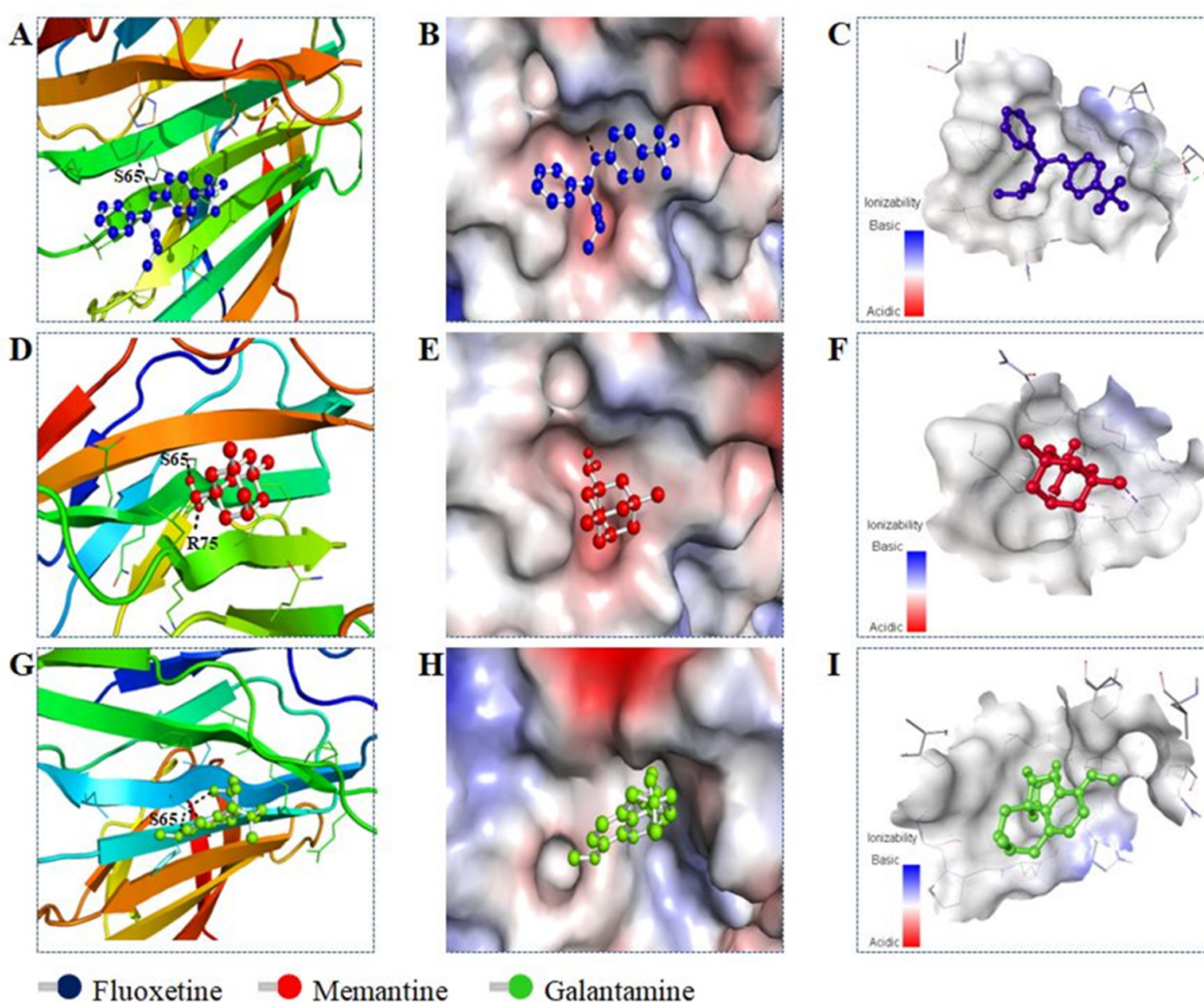


**Figure 6.** (A,D,G) Cartoon representation showing the interaction of irisin with fluoxetine, memantine, and galantamine, respectively. (B,E,H) Potential surface representation of the binding pocket and its interaction with fluoxetine, memantine and galantamine, respectively. (C,F,I) Zoomed surface view of the irisin binding pocket occupied by fluoxetine, memantine, and galantamine, respectively.

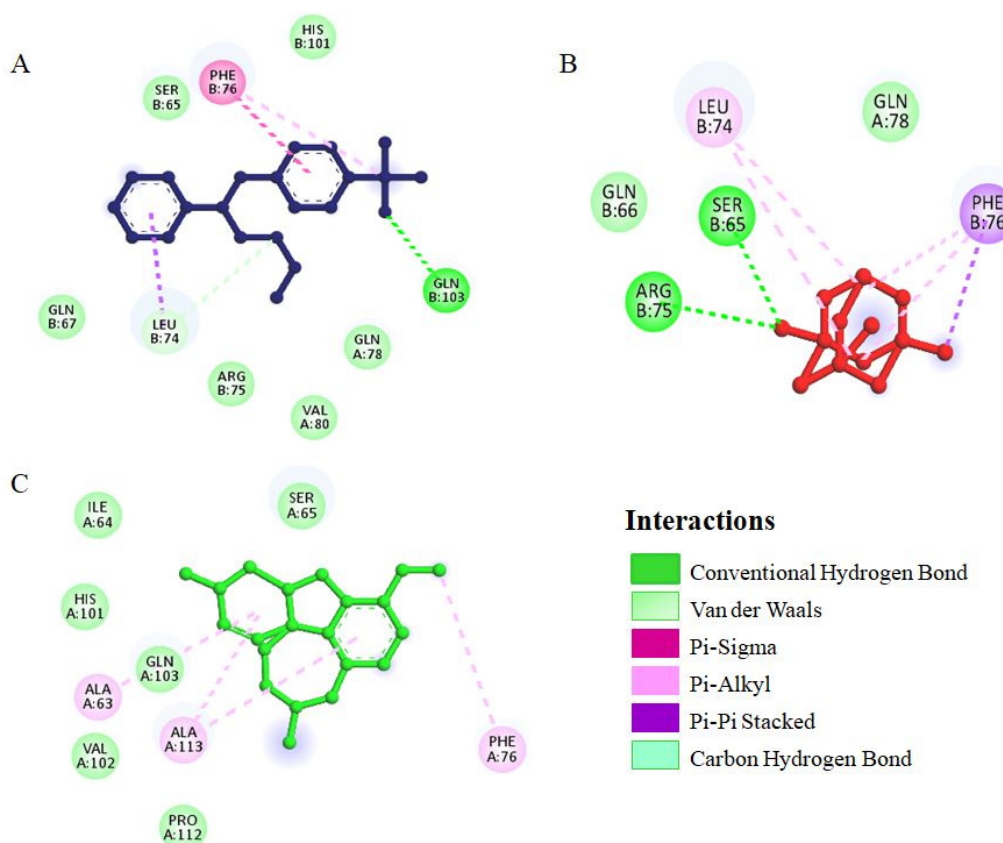


**Figure 7.** Two-dimensional structural representation of irisin residues interacting with (A) Fluoxetine (B) Memantine, and (C) Galantamine.

Figure 7B depicts 2D plot showing all the key residues of the irisin involved in interaction with memantine. Memantine was found to form two conventional hydrogen bonds with Ser65 and Arg75, highlighting the importance of this complex. Moreover, memantine showed van der Waals interaction with Gln78 of irisin. The 2D plot of irisin-galantamine interaction (Figure 7C) showed several van der Waals interactions by galantamine with Ile64, Ser65, His101, Val102, Gln102, and Pro112 of irisin. All possible docked conformers of fluoxetine, memantine, and galantamine were analyzed, and it was observed that Ser65 of irisin is a critical residue involved in the interaction with all three drugs. Both fluoxetine and memantine were found to preferentially bind with similar binding sites of irisin. Therefore, taken altogether, these docking results indicate that fluoxetine more efficiently binds with irisin as compared to memantine and galantamine, also complementing the spectroscopic results.

Therapeutic efficacy of most of these drugs is often limited by their short half-lives due to renal clearance and degradation before reaching the target site [31]. During the administration of drugs through an oral route, it is also necessary to ensure that these compounds are insoluble in the stomach, where there are several enzymes and acids that can result in substantial loss in these drugs [32]. Furthermore, these drugs must be dissolvable and should be adsorbed in the intestine through intestinal mucosa [33]. Hence, for chronic and persistent pathological conditions, there is a requirement of non-toxic, long-term, and sustainable drug delivery systems. There are several polymer materials that have been implicated in the drug delivery process in the form of nanoparticles, microcapsules, micelles, microspheres, gels, and fibers [34]. For drug delivery, interest in using protein-based biopolymers has dramatically increased in recent years due to its advantageous characteristics, including biocompatibility, biodegradability, water solubility, and non-toxicity [32]. It has been observed that natural biological molecules such as protein and



polysaccharides have excellent drug carrier system properties. The drugs, applied by any means, are transported by blood and encounter a multitude of proteins along with various cellular components. Therefore, it is predicted that using proteins or hormones in the drug delivery systems in the form of protein–drug nanoparticles, fusion proteins, or pro-drugs can be an effective therapeutic approach [35]. In the same context, an interaction study between irisin (a hormone) and AD drugs has been carried out as a preliminary study for understanding the interaction mechanism implicated in designing irisin–drug conjugates. Fluoxetine is an approved drug for AD-related symptoms and is commonly used for the treatment of anxiety and depression, and therefore it is predicted that the complex of irisin–fluoxetine can be considered as a potential candidate in the drug delivery system. Memantine also has shown significant binding with irisin, and thus is a possible binding partner of irisin. There are several proteins including transferrin and albumin that are being used as a drug carrier, so it is hypothesized that irisin can also serve as a good carrier for the delivery of drugs, as it is also known to have diverse functions in various body parts [17,26]. Moreover, investigations showed that serine residue of irisin is critically involved in interaction with all the three drugs, so it can also be implicated in designing of drug conjugates with irisin.

### 3. Materials and Methods

The irisin expression construct (*pET15b-His-3C-irisin*) was procured from Addgene (122612). For the expression of irisin, the C41-DE3 strain of *E. coli* was used. Ampicillin, memantine, galantamine, and fluoxetine were obtained from Sigma-Aldrich Co. (St. Louis, MO, USA). For buffer preparations, analytical -grade chemicals were used.

#### 3.1. Expression and Purification of Irisin

Irisin was purified according to previously published reports [26,28]. In brief, the expression construct of irisin was transformed in *E. coli* C41-DE3 cells. Maximum protein expression was obtained at 16 °C by 0.5 mM IPTG induction (18–20 h). The culture was harvested, and cells were dissolved in lysis buffer (50 mM Tris–HCl buffer pH 7.5, 300 mM NaCl, 0.5 mM  $\beta$ -mercaptoethanol, 5% (*v/v*) glycerol, and 1 mM phenyl methane sulfonyl fluoride, and centrifuged at 9000 rpm for 30 min at 4 °C. A Ni-NTA column was equilibrated and the supernatant was obtained after centrifugation was loaded on the column. The protein was eluted out at 250 mM imidazole concentration, and purity was determined on SDS-PAGE.

#### 3.2. Fluorescence Spectroscopic Measurements

The fluorescence-based assay was performed and analyzed according to previously published reports to determine the binding affinity of memantine, fluoxetine and galantamine with recombinant irisin [26,36]. The stock solutions of drugs were diluted using double distilled water. A 4  $\mu$ M concentration of irisin was used, and fluorescence measurements were taken on a Jasco spectrofluorometer FP 6200 (Jasco, Japan). The protein was excited at 280 nm, and the emission range was 300–440 nm. Both the excitation and the emission slit widths were set at 10 nm. All the spectra were reported after taking inner filter effect into consideration [37].

Fluorescence quenching of irisin was mathematically analyzed using different equations, namely, Stern–Volmer (SV) (Equation (1)) [38,39], and the double logarithmic equation (Equation (2)) [40].

#### 3.3. ITC Measurements

The binding affinities of fluoxetine, memantine, and galantamine with irisin were investigated using a VP-ITC microcalorimeter (MicroCal, Inc, GE, MicroCal, Northampton, MA, USA) at 25 °C following previously published reports [41]. The sample cell was filled with irisin solution while the three ligands were loaded into the rotator syringe. These samples were degassed before loading, and the degassing was carried out in a thermovac

chamber for 30 min. The first injection was a false one of 5  $\mu\text{L}$  followed by 10  $\mu\text{L}$  injections. Spacing was set at 280 s, and the stirring speed was kept at 307 rpm. The curve fitting was performed using different binding site models for different ligands. For irisin–fluoxetine, one site model was followed, while for irisin–memantine and irisin–galantamine, four site models were followed due to the best fitting obtained for the isotherm, as followed in previously published literature [42,43]. The final figure was obtained using the MicroCal Origin 8.0 software to find the association constant ( $K_a$ ), entropy change ( $\Delta S$ ), and enthalpy change ( $\Delta H$ ).

### 3.4. Molecular Docking

To have insight into the interaction pattern between irisin and drugs, molecular docking was performed. Bioinformatics tools such as PyMOL [44], MGL Tools [45], AutoDock Vina [46], and Discovery Studio [47] were employed for docking and analysis. The structure of irisin was obtained from the Protein Data Bank (PDB-ID-4LSD) in a 3D state. Similarly, 3D structures of memantine, fluoxetine, and galantamine were taken in SDF format from the PubChem database. The PDB file of the receptor (irisin) and SDF files of ligands (drugs) were converted into PDBQT format to perform docking. The ligand structures and receptor files were used for docking by employing the AutoDock Vina software [46]. Since irisin's binding sites were not known, blind docking was performed, in which the drugs were facilitated to freely move and search for irisin. The results of the docking were saved in a separate directory, and Discovery Studio Visualizer and PyMOL tools were employed to analyze irisin–drug interactions [44,47].

## 4. Conclusions

This study examines the interaction of irisin with FDA-approved drugs for AD, which can serve as a platform for utilizing irisin as a carrier for the delivery of therapeutic drugs. In the present work, we have reported the molecular interactions of irisin with Alzheimer's drugs, namely memantine, galantamine, and fluoxetine, employing molecular docking and in vitro binding studies. It has been observed from spectroscopic and molecular docking studies that significant binding occurred between irisin and these drugs, with fluoxetine possessing the highest binding affinity to irisin. Fluorescence quenching revealed that fluoxetine binds to irisin with a high affinity, i.e.,  $K = 0.21 \times 10^7 \text{M}^{-1}$  at 25 °C. ITC further revealed the associated thermodynamic and binding parameters of all three drugs with irisin, suggesting the binding to be spontaneous and exothermic. Additionally, molecular docking also validated the observations. It was found that irisin binds with all three drugs with significant affinity, and a maximum binding score (−6.3 kcal/mol) was observed for irisin–fluoxetine interaction. This study provides a platform for the use of irisin in a drug delivery system for a favorable therapeutic approach for ameliorating several diseases, owing to the various beneficial roles of irisin in the body.

**Supplementary Materials:** The following supporting information can be downloaded at: <https://www.mdpi.com/article/10.3390/ijms23115965/s1>.

**Author Contributions:** R.W.—Conceptualization, experiments, formal analysis, writing—original draft, writing-review, and editing; A.S.—Data curation, visualization, methodology, ITC experiment, writing-review and editing; T.K.—Writing, methodology, and editing; M.I.H.—Investigation, Data validation; S.N.K.—Data analysis, investigation, Data validation; M.S.—Data analysis, investigation, Data validation; A.I.—Formal analysis, project administration, writing-review and editing, Data analysis, project administration. All authors have read and agreed to the published version of the manuscript.

**Funding:** By the Indian Council of Medical Research ISRM/12/(127)/2020 and (45/39/2018-BIO/BMS).

**Institutional Review Board Statement:** Not applicable.

**Informed Consent Statement:** Not applicable.

**Data Availability Statement:** All the data have been provided in the manuscript.

**Acknowledgments:** This work was supported by a grant from the Indian Council of Medical Research ISRM/12/(127)/2020 and (45/39/2018-BIO/BMS). The authors are grateful to the FIST Program (SR/FST/LSI-541/2012) and Jamia Millia Islamia (a Central University) for providing all the necessary facilities to carry out this work. A.S. is thankful to the UGC for D.S. Kothari Postdoctoral fellowship ((BSR)/BL/19-20/0119). R.W. acknowledges DST-INSPIRE for INSPIRE Fellowship (IF-180728). The authors acknowledge the College of Medicine and Deanship of scientific research, Prince Sattam bin Abdul-Aziz University, Alkharj, K.S.A. for their continuous support in carrying out this research.

**Conflicts of Interest:** All authors declare that they have no conflict of interest.

## References

1. Waseem, R.; Shamsi, A.; Kazim, S.N.; Islam, A. An insight into mitochondrial dysfunction and its implications in neurological diseases. *Curr. Drug Targets* **2021**, *22*, 1585–1595. [\[CrossRef\]](#) [\[PubMed\]](#)
2. Cummings, J.L.; Tong, G.; Ballard, C. Treatment combinations for Alzheimer's disease: Current and future pharmacotherapy options. *J. Alzheimer's Dis.* **2019**, *67*, 779–794. [\[CrossRef\]](#) [\[PubMed\]](#)
3. Goedert, M.; Spillantini, M.G. A century of Alzheimer's disease. *Science* **2006**, *314*, 777–781. [\[CrossRef\]](#) [\[PubMed\]](#)
4. Hung, S.-Y.; Fu, W.-M. Drug candidates in clinical trials for Alzheimer's disease. *J. Biomed. Sci.* **2017**, *24*, 47. [\[CrossRef\]](#) [\[PubMed\]](#)
5. Gong, C.-X.; Liu, F.; Iqbal, K. Multifactorial hypothesis and multi-targets for Alzheimer's disease. *J. Alzheimer's Dis.* **2018**, *64*, S107–S117. [\[CrossRef\]](#)
6. Fish, P.V.; Steadman, D.; Bayle, E.D.; Whiting, P. New approaches for the treatment of Alzheimer's disease. *Bioorganic Med. Chem. Lett.* **2019**, *29*, 125–133. [\[CrossRef\]](#)
7. Marucci, G.; Buccioni, M.; Dal Ben, D.; Lambertucci, C.; Volpini, R.; Amenta, F. Efficacy of acetylcholinesterase inhibitors in Alzheimer's disease. *Neuropharmacology* **2021**, *190*, 108352. [\[CrossRef\]](#)
8. Yoo, J.-W.; Irvine, D.J.; Discher, D.E.; Mitragotri, S. Bio-inspired, bioengineered and biomimetic drug delivery carriers. *Nat. Rev. Drug Discov.* **2011**, *10*, 521–535. [\[CrossRef\]](#)
9. Ha, D.; Yang, N.; Nadithe, V. Exosomes as therapeutic drug carriers and delivery vehicles across biological membranes: Current perspectives and future challenges. *Acta Pharm. Sin. B* **2016**, *6*, 287–296. [\[CrossRef\]](#)
10. Kratz, F.; Ehling, G.; Kauffmann, H.; Unger, C. Acute and repeat-dose toxicity studies of the (6-maleimidocaproyl) hydrazone derivative of doxorubicin (DOXO-EMCH), an albumin-binding prodrug of the anticancer agent doxorubicin. *Hum. Exp. Toxicol.* **2007**, *26*, 19–35. [\[CrossRef\]](#)
11. Wenk, E.; Merkle, H.P.; Meinel, L. Silk fibroin as a vehicle for drug delivery applications. *J. Control. Release* **2011**, *150*, 128–141. [\[CrossRef\]](#) [\[PubMed\]](#)
12. Szwed, M.; Matusiak, A.; Laroche-Clary, A.; Robert, J.; Marszalek, I.; Jozwiak, Z. Transferrin as a drug carrier: Cytotoxicity, cellular uptake and transport kinetics of doxorubicin transferrin conjugate in the human leukemia cells. *Toxicol. Vitro.* **2014**, *28*, 187–197. [\[CrossRef\]](#) [\[PubMed\]](#)
13. Lourenco, M.V.; Frozza, R.L.; de Freitas, G.B.; Zhang, H.; Kincheski, G.C.; Ribeiro, F.C.; Gonçalves, R.A.; Clarke, J.R.; Beckman, D.; Staniszewski, A. Exercise-linked FNDC5/irisin rescues synaptic plasticity and memory defects in Alzheimer's models. *Nat. Med.* **2019**, *25*, 165–175. [\[CrossRef\]](#)
14. Waseem, R.; Shamsi, A.; Mohammad, T.; Hassan, M.; Kazim, S.N.; Chaudhary, A.A.; Rudayni, H.A.; Al-Zharani, M.; Ahmad, F.; Islam, A. FNDC5/Irisin: Physiology and Pathophysiology. *Molecules* **2022**, *27*, 1118. [\[CrossRef\]](#) [\[PubMed\]](#)
15. Peng, J.; Deng, X.; Huang, W.; Yu, J.-H.; Wang, J.-X.; Wang, J.-P.; Yang, S.-B.; Liu, X.; Wang, L.; Zhang, Y. Irisin protects against neuronal injury induced by oxygen-glucose deprivation in part depends on the inhibition of ROS-NLRP3 inflammatory signaling pathway. *Mol. Immunol.* **2017**, *91*, 185–194. [\[CrossRef\]](#) [\[PubMed\]](#)
16. Wrann, C.D.; White, J.P.; Salogiannis, J.; Laznik-Bogoslavski, D.; Wu, J.; Ma, D.; Lin, J.D.; Greenberg, M.E.; Spiegelman, B.M. Exercise induces hippocampal BDNF through a PGC-1 $\alpha$ /FNDC5 pathway. *Cell Metab.* **2013**, *18*, 649–659. [\[CrossRef\]](#)
17. Noda, Y.; Kuzuya, A.; Tanigawa, K.; Araki, M.; Kawai, R.; Ma, B.; Sasakura, Y.; Maesako, M.; Tashiro, Y.; Miyamoto, M. Fibronectin type III domain-containing protein 5 interacts with APP and decreases amyloid  $\beta$  production in Alzheimer's disease. *Mol. Brain* **2018**, *11*, 61. [\[CrossRef\]](#)
18. Jiang, J.; Jiang, H. Efficacy and adverse effects of memantine treatment for Alzheimer's disease from randomized controlled trials. *Neurol. Sci.* **2015**, *36*, 1633–1641. [\[CrossRef\]](#)
19. Alhumaydhi, F.A.; Aljasir, M.A.; Aljohani, A.S.; Alsagaby, S.A.; Alwashmi, A.S.; Shahwan, M.; Hassan, M.I.; Islam, A.; Shamsi, A. Probing the interaction of memantine, an important Alzheimer's drug, with human serum albumin: In silico and in vitro approach. *J. Mol. Liq.* **2021**, *340*, 116888. [\[CrossRef\]](#)
20. Tariot, P. Current status and new developments with galantamine in the treatment of Alzheimer's disease. *Expert Opin. Pharmacother.* **2001**, *2*, 2027–2049. [\[CrossRef\]](#)
21. Khan, M.S.; Husain, F.M.; Alhumaydhi, F.A.; Alwashmi, A.S.; Rehman, M.T.; Alruwetei, A.M.; Hassan, M.I.; Islam, A.; Shamsi, A. Exploring the molecular interactions of Galantamine with human Transferrin: In-silico and in vitro insight. *J. Mol. Liq.* **2021**, *335*, 116227. [\[CrossRef\]](#)
22. Benfield, P.; Heel, R.C.; Lewis, S.P. Fluoxetine. *Drugs* **1986**, *32*, 481–508. [\[CrossRef\]](#) [\[PubMed\]](#)

23. Khan, M.S.; Shahwan, M.; Shamsi, A.; Alhumaydhi, F.A.; Alsagaby, S.A.; Al Abdulmonem, W.; Abdullaev, B.; Yadav, D.K. Elucidating the Interactions of Fluoxetine with Human Transferrin Employing Spectroscopic, Calorimetric, and In Silico Approaches: Implications of a Potent Alzheimer's Drug. *ACS Omega* **2022**, *7*, 9015. [CrossRef] [PubMed]
24. Waseem, R.; Anwar, S.; Khan, S.; Shamsi, A.; Hassan, M.; Anjum, F.; Shafie, A.; Islam, A.; Yadav, D.K. MAP/Microtubule Affinity Regulating Kinase 4 Inhibitory Potential of Irisin: A New Therapeutic Strategy to Combat Cancer and Alzheimer's Disease. *Int. J. Mol. Sci.* **2021**, *22*, 10986. [CrossRef] [PubMed]
25. Shamsi, A.; Mohammad, T.; Khan, M.S.; Shahwan, M.; Husain, F.M.; Rehman, M.; Hassan, M.; Ahmad, F.; Islam, A. Unraveling binding mechanism of Alzheimer's drug rivastigmine tartrate with human transferrin: Molecular docking and multi-spectroscopic approach towards neurodegenerative diseases. *Biomolecules* **2019**, *9*, 495. [CrossRef]
26. Waseem, R.; Shamsi, A.; Mohammad, T.; Alhumaydhi, F.A.; Kazim, S.N.; Hassan, M.I.; Ahmad, F.; Islam, A. Multispectroscopic and Molecular Docking Insight into Elucidating the Interaction of Irisin with Rivastigmine Tartrate: A Combinational Therapy Approach to Fight Alzheimer's Disease. *ACS Omega* **2021**, *6*, 7910–7921. [CrossRef]
27. Lakowicz, J.R. Quenching of fluorescence. In *Principles of Fluorescence Spectroscopy*; Springer: Boston, MA, USA, 1983; pp. 257–301.
28. Waseem, R.; Shamsi, A.; Shahbaz, M.; Khan, T.; Kazim, S.N.; Ahmad, F.; Hassan, M.I.; Islam, A. Effect of pH on the structure and stability of irisin, a multifunctional protein: Multispectroscopic and molecular dynamics simulation approach. *J. Mol. Struct.* **2022**, *1252*, 132141. [CrossRef]
29. Shamsi, A.; Al Shahwan, M.; Ahamad, S.; Hassan, M.I.; Ahmad, F.; Islam, A. Spectroscopic, calorimetric and molecular docking insight into the interaction of Alzheimer's drug donepezil with human transferrin: Implications of Alzheimer's drug. *J. Biomol. Struct. Dyn.* **2020**, *38*, 1094–1102. [CrossRef]
30. Anwar, S.; Shamsi, A.; Shahbaaz, M.; Queen, A.; Khan, P.; Hasan, G.M.; Islam, A.; Alajmi, M.F.; Hussain, A.; Ahmad, F. Rosmarinic acid exhibits anticancer effects via MARK4 inhibition. *Sci. Rep.* **2020**, *10*, 10300. [CrossRef]
31. Bae, K.H.; Lee, F.; Xu, K.; Keng, C.T.; Tan, S.Y.; Tan, Y.J.; Chen, Q.; Kurisawa, M. Microstructured dextran hydrogels for burst-free sustained release of PEGylated protein drugs. *Biomaterials* **2015**, *63*, 146–157. [CrossRef]
32. Garrait, G.; Beyssac, E.; Subirade, M. Development of a novel drug delivery system: Chitosan nanoparticles entrapped in alginate microparticles. *J. Microencapsul.* **2014**, *31*, 363–372. [CrossRef] [PubMed]
33. Hubbell, J.A.; Chilkoti, A. Nanomaterials for drug delivery. *Science* **2012**, *337*, 303–305. [CrossRef]
34. Jao, D.; Xue, Y.; Medina, J.; Hu, X. Protein-based drug-delivery materials. *Materials* **2017**, *10*, 517. [CrossRef]
35. Kratz, F.; Elsadek, B. Clinical impact of serum proteins on drug delivery. *J. Control. Release* **2012**, *161*, 429–445. [CrossRef] [PubMed]
36. Shamsi, A.; Ahmed, A.; Bano, B. Probing the interaction of anticancer drug temsirolimus with human serum albumin: Molecular docking and spectroscopic insight. *J. Biomol. Struct. Dyn.* **2018**, *36*, 1479–1489. [CrossRef] [PubMed]
37. Chi, Z.; Liu, R. Phenotypic characterization of the binding of tetracycline to human serum albumin. *Biomacromolecules* **2011**, *12*, 203–209. [CrossRef] [PubMed]
38. Valeur, B. *Molecular Fluorescence: Principles and Applications*; John Wiley & Sons: Hoboken, NJ, USA, 2002.
39. Lakowicz, J.R. *Principles of Fluorescence Spectroscopy*; Springer US: Boston, MA, USA, 2006.
40. Feng, X.-Z.; Lin, Z.; Yang, L.-J.; Wang, C.; Bai, C.-L. Investigation of the interaction between acridine orange and bovine serum albumin. *Talanta* **1998**, *47*, 1223–1229. [CrossRef]
41. Anwar, S.; DasGupta, D.; Shafie, A.; Alhumaydhi, F.A.; Alsagaby, S.A.; Shahwan, M.; Anjum, F.; Al Abdulmonem, W.; Sharaf, S.E.; Hassan, M.I. Implications of Tempol in Pyruvate Dehydrogenase Kinase 3 Targeted Anticancer therapeutics: Computational, Spectroscopic and Calorimetric Studies. *J. Mol. Liq.* **2022**, *350*, 118581. [CrossRef]
42. Shamsi, A.; Mohammad, T.; Anwar, S.; Alajmi, M.F.; Hussain, A.; Hassan, M.I.; Ahmad, F.; Islam, A. Probing the interaction of Rivastigmine Tartrate, an important Alzheimer's drug, with serum albumin: Attempting treatment of Alzheimer's disease. *Int. J. Biol. Macromol.* **2020**, *148*, 533–542. [CrossRef]
43. Yousuf, M.; Shamsi, A.; Queen, A.; Shahbaaz, M.; Khan, P.; Hussain, A.; Alajmi, M.F.; Rizwanul Haque, Q.M.; Imtaiyaz Hassan, M. Targeting cyclin-dependent kinase 6 by vanillin inhibits proliferation of breast and lung cancer cells: Combined computational and biochemical studies. *J. Cell. Biochem.* **2021**, *122*, 897–910. [CrossRef]
44. DeLano, W.L. The PyMOL Molecular Graphics System. 2002. Available online: <http://www.pymol.org> (accessed on 12 May 2022).
45. Jacob, R.B.; Andersen, T.; McDougal, O.M. Accessible high-throughput virtual screening molecular docking software for students and educators. *PLoS Comput. Biol.* **2012**, *8*, e1002499. [CrossRef] [PubMed]
46. Trott, O.; Olson, A.J. AutoDock Vina: Improving the speed and accuracy of docking with a new scoring function, efficient optimization, and multithreading. *J. Comput. Chem.* **2010**, *31*, 455–461. [CrossRef] [PubMed]
47. Biovia, D.S. *Discovery Studio Modeling Environment, Release 4.5*; Dassault Systèmes Biovia: San Diego, CA, USA, 2015.